Influence of a strong sample solvent on analyte dispersion in chromatographic columns

Manoranjan Mishra [a,*], Chinar Rana [a], A. De Wit [b], Michel Martin [c]

[a] Department of Mathematics, Indian Institute of Technology Ropar, 140001 Rupnagar, India
[b] Nonlinear Physical Chemistry Unit, Service de Chimie Physique et Biologie Théorique, Faculté des Sciences, CP 231, Université Libre de Bruxelles (ULB), 1050 Brussels, Belgium
[c] Ecole Supérieure de Physique et de Chimie Industrielles, Laboratoire de Physique et Mécanique des Milieux Hétérogènes (PMMH, UMR 7636 CNRS, ESPCI-ParisTech, Université Pierre et Marie Curie, Université Paris-Diderot), 10 rue Vauquelin, 75231 Paris Cedex 05, France

ABSTRACT

In chromatographic columns, when the eluting strength of the sample solvent is larger than that of the carrier liquid, a deformation of the analyte zone occurs because its frontal part moves at a relatively high velocity due to a low retention factor in the sample solvent while the rear part of the analyte zone is more retained in the carrier liquid and hence moves at a lower velocity. The influence of this solvent strength effect on the separation of analytes is studied here theoretically using a mass balance model describing the spatio-temporal evolution of the eluent, the sample solvent and the analyte. The viscosity of the sample solvent and carrier fluid is supposed to be the same (i.e. no viscous fingering effects are taken into account). A linear isotherm adsorption with a retention factor depending upon the local concentration of the liquid phase is considered. The governing equations are numerically solved by using a Fourier spectral method and parametric studies are performed to analyze the effect of various governing parameters on the dispersion and skewness of the analyte zone. The distortion of this zone is found to depend strongly on the difference in eluting strength between the mobile phase and the sample solvent as well as on the sample volume.

1. Introduction

In liquid chromatography, samples are introduced in the liquid state. The sample components are therefore injected in solution either in the solvent in which they are originally found or in the solvent used in the last step of the sample preparation procedure. During their migration through the chromatographic column, the analytes are in contact with two solvents, the sample solvent and the mobile phase (the composition of which may vary with time in case of a gradient elution operation). Because these solvents may not themselves be pure liquids, but may be mixtures of two or more solvents or of a solvent and some additives (e.g. ionic compounds), one may better describe them as solvent systems.

It has been observed, in reversed-phase liquid chromatography (RPLC), that analyte peaks are sometimes broadened, distorted or even split when the two solvent systems are different in nature. This occurs in isocratic elution [1–8] as well as in gradient elution [9,10], and can also happen in hydrophilic interaction liquid chromatography [11]. This is detrimental to the separation performance. These

observations have led to recommend the use of the mobile phase (or of the initial mobile phase in the case of gradient elution) as the sample solvent [12–14]. However, this is not always feasible for a variety of reasons, for instance when the analytes of interest have a low solubility in the mobile phase.

Two physico-chemical parameters of solvent systems have been recognized as responsible for the analyte peak shape perturbations when their values in the mobile phase and in the sample solvent differ: the viscosity and the solvent strength (or eluting strength), the latter reflecting the ability of the liquid to displace the analytes from a particular stationary phase and thus to decrease their retention.

The viscosity effect is linked to a hydrodynamic instability which occurs when a less viscous fluid displaces a more viscous one in a porous medium or in a conduit. Any perturbation of the interface between the two fluids gets amplified and the initially planar interface becomes wavy and takes progressively the shape of fingers, hence the name viscous fingering given to this phenomenon. In chromatography, the sample is surrounded by the mobile phase and the development of this hydrodynamic instability can occur at the upstream sample/carrier liquid interface if the sample is more viscous than the eluent or at the downstream interface in the opposite case. Although the potentially harmful character of the viscous fingering effect in chromatography was

* Corresponding author. Tel.: +91 9501705522.
E-mail addresses: manoranjan.mishra@gmail.com, manoranjan@iitrpr.ac.in (M. Mishra).

recognized in the early literature on size exclusion chromatography in which highly viscous polymeric samples are injected (see Introduction of Ref. [15] for a historical review of this recognition), it is more recently, in the two last decades, that this effect was considered for analytical chromatographic separations of relatively small molecular components [15–26].

The solvent strength effect arises from a difference in the values of the solvent strength parameter of the eluent and of the sample solvent. Then, the retention factor, k, of a given analyte does not take the same value in these two solvent systems. Consequently, its migration velocity, which is proportional to $1/(1 + k)$, is not the same when it is dissolved in the sample solvent system as when it is surrounded by the mobile phase. When the analyte retention factor in the sample solvent is very large, this effect might be beneficial since the leading front of the analyte zone moves very slowly during the injection process and the column volume occupied by the analyte zone at the end of this injection process can be much smaller than the injected sample volume. This effect is taken to profit for analyzing components present in trace amounts in the sample. Indeed, very large sample volumes can then be introduced in the column, which leaves a sufficiently large amount of these trace analytes in the column for leading to high enough detection signal-to-noise ratios at the column outlet and precise enough quantitative analysis [27–37]. If, instead, the sample solvent is stronger than the mobile phase, the analyte migration velocity in the sample solvent is larger than in the mobile phase. Since the leading front of the analyte zone moves faster than its rear front, the analyte zone is stretched, which leads to increased peak broadening and possible distortion of the peak shape. It is for avoiding these disturbances that it has been recommended that the mobile phase be chosen as the sample solvent [12–14], or even that the latter be weaker than the mobile phase [38].

In practice, when the sample solvent and the mobile phase are of different nature or composition, the viscosity effect and the solvent strength effect are likely to occur simultaneously. Their interplay and their overall influence on analyte zone migration and peak shape are complex, the more so as these two solvent systems are undergoing intermixing during their transport through the column both at the leading and rear fronts of the sample solvent zone. Still, for optimizing separations in which these two solvent systems are different, a quantitative description of the influence of these solvent effects, taken individually as well as in combination, is required. The quantitative influence of the various parameters controlling viscous fingering on analyte peak characteristics has been investigated in various chromatographic situations (unretained as well as retained analytes, positive as well as negative viscosity contrast between sample and eluent, analytes with a negligible or significant intrinsic viscosity) by means of numerical simulations [15,24–26,39–41].

To our knowledge, there has been only one attempt to quantitatively address the solvent strength effect using computer simulations [42]. However, because of computing capacity limitations, the computer program used did not take into account the dispersion of the analyte and sample solvent zones as they advance through the column, so that the analyte retention factor was taking one of only two values, that in the pure mobile phase and that in the pure sample solvent. Therefore, although peak distortion and splitting could be simulated, the simulations could not match the actual process occurring within the column where the dispersive mixing of the sample solvent and of the mobile phase affects the behavior of the analyte.

The purpose of the present study is to investigate the quantitative aspects of the solvent strength effect when the sample solvent is stronger than the mobile phase. This is performed by means of numerically simulating the dispersion of the analyte and sample solvent zones and taking into account the dependence of the
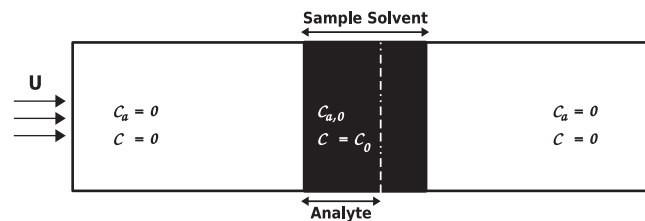

Fig. 1. Sketch of the system at initial time, i.e. at the end of the injection process. The contour rectangle schematically represents a fraction of the length of the column. Because of its slight retention in the sample solvent, the width of the analyte zone is shorter than that of the sample solvent zone. The positions of the rear (left) fronts of both zones are the same.

analyte retention factor on the local composition of the mixture of eluent and sample solvent, which evolves in time and distance along the column. It is assumed that the viscosities of the mobile phase and of the sample solvent are the same, i.e. viscous fingering does not occur in the column.

Besides the viscosity and solvent strength effects described above, additional effects may affect the analyte zone patterns when the sample solvent differs from the mobile phase and perturb the separation. For instance, a limited solubility in the mobile phase may lead to precipitation or crystallization of the analyte in the connection tubes or in the column. In the current study, it is assumed that such effects do not occur in the simulations.

2. Mathematical model

We consider the displacement of a given sample volume within a reversed-phase liquid chromatographic column (see Fig. 1). This sample volume of finite width W consisting of a solute or analyte in concentration $c_{a,0}$ dissolved in a solvent which is a mixture of an organic modifier (typically, methanol or acetonitrile) and water with volume fraction ϕ_s in organic modifier is injected at initial time $t = 0$ in the column. Although, in real chromatographic systems, the injection port may induce some distortion and cross-sectional non-uniformities in the initial concentration profiles of the sample solvent and analyte zones, the uniform rectangular profiles shown in Fig. 1 are selected for investigating the genuine influence of the sample solvent effect. This sample is displaced by the eluent with a mean velocity U along the x direction. The eluent is also a mixture of the same organic modifier and water with volume fraction ϕ_m in organic modifier. We assume that the initial analyte concentration $c_{a,0}$ in the sample solvent is small (i.e. diluted enough) and that it does not influence the fluid viscosity. Furthermore, because we want to study the sole solvent strength effect, the fluid viscosity does not play a role in our model and we assume that viscous fingering does not occur.

The sample solvent is not retained by the stationary phase. However, the analyte dissolved in it is retained following the reversible adsorption–desorption reaction

$$A_m \underset{k_d}{\overset{k_a}{\rightleftharpoons}} A_s. \tag{1}$$

Here A_m and A_s represent the analyte molecules in the mobile and stationary phases where their concentrations are equal to $c_{a,m}$ and $c_{a,s}$ respectively, while k_a and k_d are the adsorption and desorption kinetic constants. The analyte retention is characterized by the retention factor $k = FK$, where $F = V_s/V_m = (1 - \epsilon_{tot})/\epsilon_{tot}$ is the phase ratio of the volume V_s and V_m of the stationary and mobile phases, where ϵ_{tot} is the total porosity or void volume fraction of the porous medium, and $K = k_a/k_d$ is the equilibrium constant of the adsorption–desorption equilibrium [43].

In the present study, we assume that the eluent and sample solvent are not isoeluotropic and hence that the analyte retention

depends on the momentary composition of the mobile phase i.e. depends explicitly on the fractional amount of the sample solvent in the eluent.

2.1. Concentration dependence of analyte retention on local liquid composition

To a first approximation, the dependence of the analyte retention factor, k, on the volume fraction, ϕ, of the organic modifier in its mixture with water is expressed by [44]:

$$\log k = \log k_0 - S\phi \tag{2}$$

where S is the solvent strength parameter, and k_0 the value of k in pure water. Typically, S has a value of about 3, which means that k in pure methanol or pure acetonitrile is about 1000 times smaller than in pure water [44]. In fact, the $\log k$ vs. ϕ relationship is better expressed by a quadratic [45] rather than by a linear relationship over the whole 0–100% range of ϕ. However, Eq. (2) can be considered as satisfactory over some restricted ϕ range. We normalize the local composition of the liquid phase as

$$c = \frac{\phi - \phi_m}{\phi_s - \phi_m} \tag{3}$$

Thus c is equal to 0 for $\phi = \phi_m$ (eluent), to 1 for $\phi = \phi_s$ (sample solvent) and takes intermediate values for mixtures of eluent and sample solvent. Since we consider the situation where the sample solvent is stronger than the eluent, $\phi_s \geq \phi_m$. Combining Eqs. (2) and (3) gives

$$\ln k = \ln k_m - S^*c \tag{4}$$

or

$$k = k_m e^{-S^*c} \tag{5}$$

with $S^* = 2.3S(\phi_s - \phi_m) = \ln(k_m/k_s)$, where k_m and k_s are the retention factors of the analyte in the eluent and in the sample solvent, respectively.

2.2. Model equations

Assuming the system to be one dimensional and that the flow velocity U of the incompressible fluid is constant, the governing mass transfer equations for the system are as follows:

$$\frac{\partial c}{\partial t} + U\frac{\partial c}{\partial x} = D_x\frac{\partial^2 c}{\partial x^2}, \tag{6}$$

$$\frac{\partial c_{a,m}}{\partial t} + F\frac{\partial c_{a,s}}{\partial t} + U\frac{\partial c_{a,m}}{\partial x} = D_{a,x}\frac{\partial^2 c_{a,m}}{\partial x^2}. \tag{7}$$

Eq. (6) is the convection–diffusion equation for the concentration c of the sample solvent. Eq. (7) is the mass balance equation for the analyte concentrations $c_{a,m}$ and $c_{a,s}$, in the mobile and stationary phases, respectively. D_x and $D_{a,x}$ are the dispersion coefficients of the sample solvent and analyte, respectively, in the displacing fluid. As a first approximation, we assume they do not depend on mobile phase liquid composition x is the distance along the flow direction and t represents the time.

Assuming a linear isotherm adsorption dependence between the concentration $c_{a,s}$ and $c_{a,m}$ as

$$c_{a,s} = Kc_{a,m} \tag{8}$$

where $K = k_a/k_d$ is the constant of the adsorption–desorption equilibrium (1) and recalling that $FK = k(c)$, Eq. (7) becomes

$$\frac{\partial c_{a,m}(1 + k(c))}{\partial t} + U\frac{\partial c_{a,m}}{\partial x} = D_{a,x}\frac{\partial^2 c_{a,m}}{\partial x^2} \tag{9}$$

The analyte concentration $c_{a,m}$ in the liquid phase varies from 0 to $c_{a,0}$.

To nondimensionalize the governing equations, we choose the concentration $c_{a,0}$ as the reference concentration for the analyte concentration in the liquid phase, and U as the characteristic velocity. Defining the length scale $L_c = D_{a,x}/U$ and a time scale $t_c = D_{a,x}/U^2$, the non dimensional quantities are then obtained as

$$\hat{x} = \frac{x}{L_c}, \quad \hat{t} = \frac{t}{t_c} \quad c_{a,m}^* = \frac{c_{a,m}}{c_{a,0}}, \quad \delta = \frac{D_x}{D_{a,x}}$$

As shown earlier [15], L_c is equal to half the plate height for the analyte and t_c to the time required to migrate this distance. Introducing a reference frame moving with the flow velocity, $x^* = \hat{x} - \hat{t}$, the governing equations with the concentration dependent retention factor become, after dropping the superscripts (*):

$$\frac{\partial c}{\partial t} = \delta\frac{\partial^2 c}{\partial x^2}, \tag{10}$$

$$\frac{\partial c_{a,m}(1 + k(c))}{\partial t} - \frac{\partial c_{a,m}k(c)}{\partial x} = \frac{\partial^2 c_{a,m}}{\partial x^2}, \tag{11}$$

$$k(c) = k_m e^{-S^*c}. \tag{12}$$

2.3. Initial and boundary conditions on analyte and sample solvent zone

In dimensionless units, the initial length of the sample zone is $l = UW/D_{a,x}$ and the middle of the sample solvent zone is set at $x = 0$. At time $t = 0$, i.e. at the end of the injection process, the analyte is retained on the porous medium. Thus the length occupied by the analyte is different from the length of the sample solvent plug. The initial analyte zone is of smaller extent than the sample solvent one and has a width $l_a = l/(1 + k_s)$ with the rear boundaries of both analyte and sample solvent at the same position $x = -l/2$. So the frontal part of the analyte zone will be at the position $l(1 - k_s)/2(1 + k_s)$ where k_s, the analyte retention factor in the pure sample solvent, has to be selected since the analyte is then surrounded by the pure sample solvent. No flux boundary conditions, which reflects mass conservation of the respective species inside the column, are assumed for the sample solvent and analyte concentration, i.e. $\partial c/\partial x$, $\partial c_{a,m}/\partial x = 0$ as $|x| \to \infty$.

2.4. Method of solutions

The objective here is to analyze the effect of $k(c)$ on the analyte peak shape by solving the model Eqs. ((10)–(12)), i.e. see how the dynamics of the sample solvent and of the analyte can disentangle because of analyte adsorption.

Eq. (10) is the classical mass diffusion equation for the sample solvent concentration. With the initial condition

$$c(x, 0) = \begin{cases} 1, & \text{for } |x| < l/2 \\ 0, & \text{for } |x| > l/2 \end{cases}$$

and the above boundary conditions, the analytical solution of Eq. (10) becomes

$$c(x, t) = \frac{1}{2}\left[\text{erf}\left(\frac{x + l/2}{\sqrt{4\delta t}}\right) + \text{erf}\left(\frac{l/2 - x}{\sqrt{4\delta t}}\right)\right]. \tag{13}$$

To simplify Eq. (11) by separating the spatial derivative and the time derivative, it can be rewritten as

$$\frac{\partial c_{a,m}}{\partial t} = \frac{1}{1 + k(c)}\left\{\frac{\partial^2 c_{a,m}}{\partial x^2} + k(c)\frac{\partial c_{a,m}}{\partial x} + S^*k(c)c_{a,m}\left(\delta\frac{\partial^2 c}{\partial x^2} - \frac{\partial c}{\partial x}\right)\right\} \tag{14}$$

With the solution $c(x, t)$ from Eq. (13) and $k(c)$ expressed as Eq. (12), the analyte mass balance evolution Eq. (14) becomes a partial differential equation with variable coefficients and cannot be solved analytically. We have hence solved this equation using a spectral method numerical technique by considering the basis function as a Fourier series.

The Fourier series expansion of $c_{a,m}(x, t)$ is taken as $c_{a,m}(x, t) = \sum_p \hat{c}_{1p}(t)e^{i(k_p x)}$, where $k_p = 2\pi p/L$ ($p = 0, 1, 2\ldots$) are the wave numbers of the Fourier modes. The Fourier coefficients $\hat{c}_{1p}$ are calculated by Fast Fourier Transform with $c_{a,m}(x, t)$ known at the collocation points $x_p = (p/M)L$, $p = 0, 1, 2, \ldots, M-1$, for M numbers of spectral modes and L is the computational length. To apply this Fourier-spectral method, periodic boundary conditions can be taken for $c_{a,m}(x, t)$ in the computational boundary, without loss of generality.

Since all the right hand side terms of Eq. (14) are with variable coefficients, for computational simplicity, we can expand them in the form of Fourier series as

$$J_1(x, t) = \frac{1}{1 + k(c)} \left\{ \frac{\partial^2 c_{a,m}}{\partial x^2} + k(c)\frac{\partial c_{a,m}}{\partial x} \right.$$

$$\left. + S^* k(c)c_{a,m} \left(\delta \frac{\partial^2 c}{\partial x^2} - \frac{\partial c}{\partial x} \right) \right\} = \sum_p \hat{J}_{1p}(t) \cdot e^{i(k_p x)}. \quad (15)$$

Then, Eq. (14) in Fourier space reduces to a first order ordinary differential equation in time,

$$\frac{d\hat{c}_{1p}}{dt} = \hat{J}_{1p}. \quad (16)$$

The solution of this equation has been found by a predictor–corrector method, where the second order Adams–Bashforth method is used to predict the concentration of the analyte. Then the predicted solution is corrected by the trapezoidal rule. In these calculations, the variable coefficient term $J_1(x, t)$ is computed at the collocation points in real space and is then Fourier transformed to obtain $\hat{J}_{1p}$. We note that a similar algorithm was also successfully used to solve the coupled equations of convection–diffusion with the Darcy's law for the viscous fingering model by Tan and Homsy [46]. The advantage of this spectral method approach over the finite difference or finite element methods is that the former one is based on the global expansion of the solution usually by high order polynomials or Fourier series, whereas the later ones are based on local representation of the functions usually by low order polynomials. A higher accuracy can be achieved in spectral methods for coarser mesh hence reducing the number of data values to store and operate upon [47].

3. Results and discussion

The aim of this study is to investigate the dispersion of the analyte in the mobile phase when the retention factor k depends locally on the relative amount, c, of the sample solvent in the mobile phase, as given by Eq. (12). To do so, we compare it to the case when the retention factor is independent of this relative amount, i.e. to the case when $S^* = 0$. The dispersion of the analyte in the mobile phase along the axial direction is shown in Fig. 2 at different times for a fixed value $k_m = 10$ and $S^* = 4.8$. This value of S^* corresponds, for instance, to an analyte injected in pure methanol and eluted with a 30–70% methanol–water mobile phase, with $S = 3$. The analyte concentration profile $c_{a,m}$ spreads more in the upstream direction (i.e. toward column inlet) and peak tailing (insert of Fig. 2) is observed. The concentration distribution $c_{a,m}$ is thus found to be bimodal, a property which is seen in practice in RPLC [1–3,5–7,9,48,49]. As time goes by, the analyte spreads to a larger region with peak tailing increasing towards the upstream direction. While Fig. 2 represents
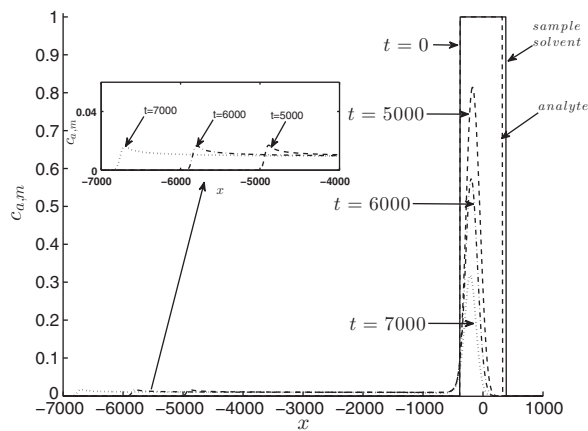

Fig. 2. Analyte concentration profiles in the liquid phase (dashed lines) as a function of x in the moving reference frame for different times with $k_m = 10$, $l = 768$, $\delta = 1$ and $S^* = 4.8$. The solid line indicates the initial concentration of sample solvent. Insert: Enlarged images of peak tailing in upstream part of the analyte profile. The upstream parts of the zones are on the left and downstream parts on the right.

the concentration distribution, along the column, of that part of the analyte present in the liquid phase, it is more instructive to represent the concentration distribution of the analyte present in both the mobile and stationary phases. This local cross-sectional average concentration is the total amount of analyte (found both in the mobile and stationary phases) in the volume of an infinitesimal slice of the column. It is proportional to $(1 + k(c))c_{a,m}$, and is plotted against x in Fig. 3. The peak tailing phenomenon is clearly observed to yield a bimodal type distribution.

In Fig. 4, the distribution, along the column, of the cross-sectional average analyte concentration is plotted for different values of k_m along the axial direction at time $t = 12,000$ after injection. The sample solvent peak corresponds to the unretained case ($k_m = 0$). The interesting observation is that the degree of retardation of the rear of the analyte zone with respect to the sample solvent zone increases with increasing k_m and so does the spreading of that zone. On the other hand, there is no such peak tailing for an unretained analyte. To understand this behavior, we note, that, locally, when surrounded by a liquid of composition c, the analyte retention factor is $k(c)$, given by Eq. (12) and the non-dimensional analyte velocity in the upstream direction in the moving frame of
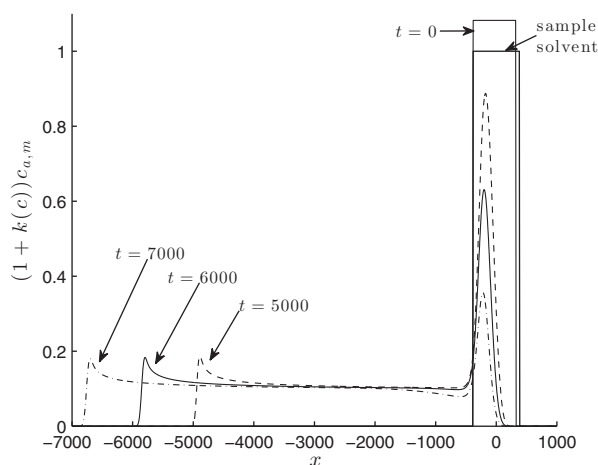

Fig. 3. Analyte cross-sectional average concentration, proportional to $(1 + k(c))c_{a,m}$ as a function of x in the moving reference frame for different times with $k_m = 10$, $l = 768$, $\delta = 1$ and $S^* = 4.8$. The upstream parts of the zones are on the left and downstream parts on the right.
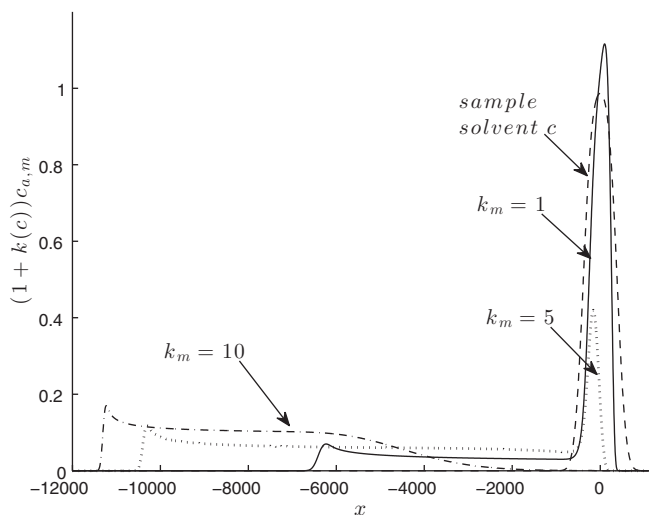
Fig. 4. Analyte cross-sectional average concentration, proportional to $(1 + k(c))c_{a,m}$, along the x-axis in the moving reference frame for different values of k_m at $t = 12{,}000$ with $S^* = 4.8$, $l = 768$, $\delta = 1$. The upstream parts of the zones are on the left and downstream parts on the right.
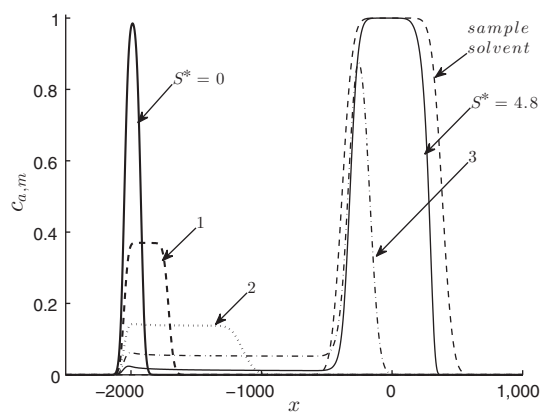

Fig. 5. Distribution of $c_{a,m}$ along the axial direction at time $t = 2000$ for different values of the solvent strength parameter S^* with $k_m = 5$, $l = 768$, $\delta = 1$. The upstream parts of the zones are on the left and downstream parts on the right.

reference is $k(c)/(1 + k(c))$, while that of the sample solvent zone is 0. The early injected analyte molecules move for some relatively long time in a liquid phase that is essentially made of the sole sample solvent, i.e. with an upstream non-dimensional advection velocity equal to $k_s/(1 + k_s)$, which is quite low since k_s is small. Instead, the analyte molecules introduced in the column at the end of the injection step, quickly surrounded by the sole mobile phase, are advected with an upstream advection velocity equal to $k_m/(1 + k_m)$, which is relatively large since k_m is large. So the upstream part of the analyte zone starts spreading swiftly once it falls behind the sample solvent zone. Besides, for the classical band broadening process associated with the analyte migration, we note that the dimensionless analyte dispersion coefficient, equal to $1/(1 + k(c))$, is larger inside the sample solvent zone than in the mobile phase because of its dependence on $k(c)$. We believe that this effect is responsible for the slight rise of the analyte cross-sectional average concentration observed near the upstream end of the analyte zone in Fig. 4.

It is also observed in Fig. 4 that, at $t = 12{,}000$, for $k_m = 10$ the analyte zone is already disengaged from the solvent zone. Then it is entirely surrounded by the mobile phase and its subsequent spreading is expected to be due to the sole classical band broadening process characterized by the dimensionless dispersion coefficient $1/(1 + k_m)$. Instead, at the same time $t = 12{,}000$, the front parts of the zones of analytes with $k_m = 5$ or 1 are still mixed with the sample solvent zone. So, the larger the retention factor k_m, the earlier the analyte disengages from the solvent zone.

In Figs. 2–4, the initial sample solvent zone width or length is selected as $l = 768$. For a 2.1 mm i.d. column packed with 1.7 μm particles with a total porosity of 0.7 and operated at a reduced plate height of 3 for the analyte, this corresponds to an injected sample volume of 5 μL.

3.1. Effect of the difference in solvent strength between sample solvent and mobile phase

The distribution, along the column, of the analyte present in the liquid phase is shown in Fig. 5, at a fixed time $t = 2000$ for $k_m = 5$ and different values of S^*, $S^* = 0$, 1, 2, 3, and 4.8, which, if $S = 3$, corresponds to $\phi_s - \phi_m = 0\%$, 15%, 29%, 43% and 70%, respectively. For the isoeluotropic solvent case, $S^* = 0$, the retention factor k is independent of concentration c and equals k_m. Fig. 5 at $t = 2000$

shows that, in that case, the analyte is well disengaged from the sample solvent, since the time of disengagement between analyte and sample solvent equals $t = 1786$ (calculated from Eq.(22) of the model by Mishra et al. [24]). Further, for larger values of $S^* = 3$, 4.8, the presence of the analyte is observed inside the sample solvent zone while, for $S^* = 1$, 2, the analyte zones are already disengaged from the sample solvent zone. It is observed that, in the case of non-isoeluotropic solvent $S^* > 0$, the rear part of the analyte zone outside the sample solvent zone follows a similar pattern as that in the case $S^* = 0$. It lags behind by the same distance from the sample solvent as in the case of isoeluotropic samples and a peak occurs at the same position but is reduced in amplitude for $S^* > 0$ as indicated in Fig. 5. Moreover, the analyte travels with the sample solvent for a much longer time in non-isoeluotropic sample solvent as compared to the isoeluotropic case. Thus an increase of the solvent strength parameter S^* induces a delay in the disengagement of the analyte zone from the sample solvent zone.

3.2. Displacement without dispersion of the sample solvent

Finding an analytical solution to Eq. (11) for the analyte concentration profile is impossible. This is why numerical simulations were needed to plot Figs. 4 and 5. They illustrate the fact that the distortion of the analyte zone occurs when a part of this zone is in contact with the sample solvent zone. Below, a simplified theoretical model is developed to estimate the critical time, t_{crit}, at which the analyte zone is disengaged from the sample solvent zone. This model is simplified since the sample solvent zone is assumed to be displaced without dispersion. The analyte and sample solvent concentration profiles cease to overlap when the position of the rear interface of the sample solvent $x_{s,r}$ will be ahead of the frontal interface of the solute zone $x_{a,f}$. In this model, the sample solvent plug remains of constant shape in time and only the analyte propagates with dispersion. Thus in the moving reference frame, the concentration c of the sample solvent remains constant and equals 0 in the eluent and 1 in the sample solvent. Since l is the length of the sample solvent zone and its middle is at $x = 0$, its rear interface is located at $x = -(l/2)$ at all times in the moving frame. Therefore, in the steady frame of reference the positions of the rear interface of the solvent and the frontal interface of the analyte are given by:

$$x_{s,r} = -\frac{l}{2} + t \tag{17}$$

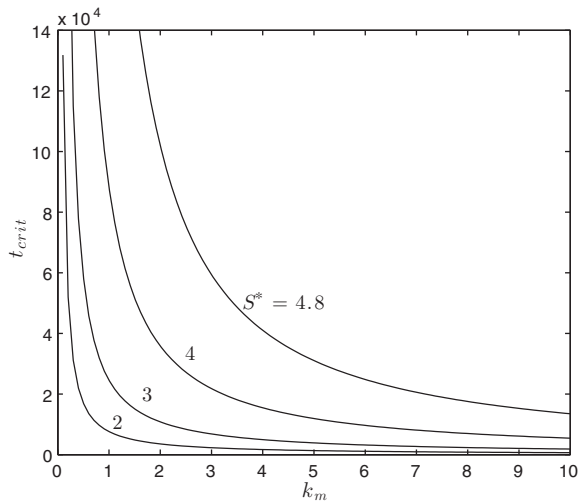$$x_{a,f} = \frac{l(1 - k_s)}{2(1 + k_s)} + \frac{t}{1 + k_s} + 2\sigma_a(t) \tag{18}$$

Fig. 6. Critical time t_{crit} at which the analyte zone ceases to overlap with the non-dispersed sample solvent one as a function of k_m for different values of S^*.

where $2\sigma_a(t)$ is the increase due to dispersion. Equating $x_{s,r}$ with $x_{a,f}$ we get

$$\frac{k_s}{1+k_s}t_{crit} - 2\sqrt{2}\sqrt{\frac{1}{1+k_s}}\sqrt{t_{crit}} - \frac{l}{1+k_s} = 0 \qquad (19)$$

This above equation gives two roots for t_{crit} and has one unique solution only by considering the root with positive sign of square root of the discriminant. Hence the corresponding critical time is

$$t_{crit} = \frac{1+k_s}{k_s^2}\left(\sqrt{2} + \sqrt{2 + \frac{lk_s}{1+k_s}}\right)^2 \qquad (20)$$

Thus t_{crit} is solely a function of l and k_s, hence of l, k_m and S^*.

In Fig. 6, t_{crit} is plotted as a function of k_m for different values of S^* keeping l constant. It is observed that the larger k_m, the smaller t_{crit}. Moreover with an increase in the solvent strength parameter S^*, t_{crit} increases. For $k_m = 1$, $l = 768$, $S^* = 2$ one can obtain from Eq. (20) that disengagement of the retained solute and of the sample solvent occurs at $t = 7618.5$. However by taking $S^* = 0$, i.e. for the isoeluotropic sample solvent, it occurs at $t = 887.13$ which is much smaller than for the non-isoeluotropic case. Thus the dependence of the retention factor on the concentration of the sample solvent induces a delay in the disengagement of the solute from solvent plugs. In the limiting case when k_s goes to ∞ i.e for very large values of k_s, t_{crit} goes to zero and when k_s goes to zero, t_{crit} becomes very large.

In Fig. 7, the time of disengagement of the analyte from the sample solvent zone is plotted as a function of the length l of the sample solvent plug for different values of S^*. It is observed that with an increase in length of the sample solvent, t_{crit} increases which implies that more time is required for disengagement of the analyte from the sample solvent for large sample volumes. Moreover, this t_{crit} increases further with an increase in the sample solvent strength parameter S^*.

3.3. Variance of the analyte zone

To quantify the effect of non-isoeluotropic sample solvents on the dispersion of analytes in chromatographic columns, we next compute the variance of the cross sectional average concentration
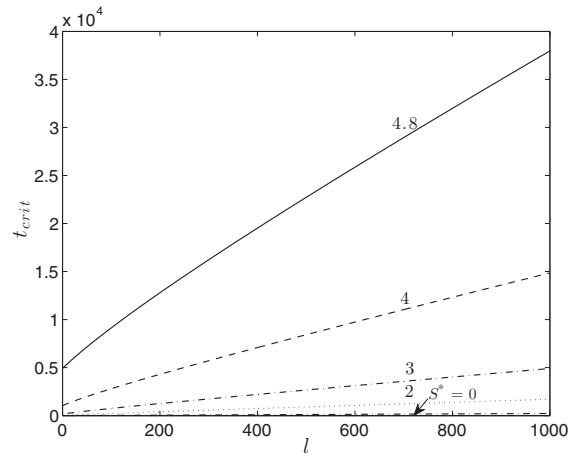

Fig. 7. Critical time of disengagement of the analyte and sample solvent zones as a function of initial length of the sample solvent plug (proportional to the injected sample volume) for different values of S^* at $k_m = 5$.

of the analyte which is proportional to $(1 + k(c))c_{a,m}$. This variance, σ_a^2, tells about the width of the distribution and is given by

$$\sigma_a^2(t) = \frac{\int_0^L (1 + k(c))c_{a,m}(x,t)[x - m(t)]^2 dx}{\int_0^L (1 + k(c))c_{a,m}(x,t)dx} \qquad (21)$$

where $m(t) = \int_0^L xf(x,t)dx$ is the first moment of $f(x,t)$, where

$$f(x,t) = \frac{(1 + k(c))c_{a,m}(x,t)}{\int_0^L (1 + k(c))c_{a,m}(x,t)dx}$$

is the probability density function of the continuous distribution of the analyte cross-sectional average concentration.

As discussed in previous studies on dispersion phenomena in chromatographic columns [39,24] the variance of the solvent zone is $\sigma_0^2 = l^2/12 + 2\delta t$ and that of an analyte dissolved in the mobile phase is $\sigma_{a,0}^2 = l_a^2/12 + 2[1/(1+k_m)]t$, where $l^2/12$ and $l_a^2/12$ are the contributions due to the initial widths of the sample solvent and of the analyte zones respectively. The variances due to the dispersion during the migration along the column are $2\delta t$ and $2[1/(1+k_m)]t$ for the zones of the sample solvent and of the analyte injected in the mobile phase, respectively. In order to quantify the effect of sample solvent strength on the variance of the analyte, we extract the quantity $\sigma_{a,s}^2 = \sigma_a^2 - \sigma_{a,0}^2$. Here $\sigma_{a,s}^2$ quantifies the contribution of the solvent strength effect, reflected in S^*, to the analyte variance.

The influences of the retention factor k_m and solvent strength parameter S^* on the total variance of analyte cross-sectional average concentration are shown in Fig. 8(a) and (b) respectively. As the initial length of the analyte zone depends upon k_s, thus upon S^* and k_m, so does its contribution to the analyte variance. The curve for $k_m = 10$ in Fig. 8(a) reflects the variance of the distributions presented in Fig. 3. It is observed that the variance increases first gradually (insert of Fig. 8(a)), then reaches a point where it increases much more slowly with time. This point corresponds to the critical time discussed above. It is noticeable that, due to the solvent strength effect, the variance for a retained analyte is at all times much larger than it would be for an unretained analyte (in which case the solvent strength effect vanishes). In the early stages of the migration process, the larger k_m, the larger the rate of increase of the analyte variance. However, since the critical time of disengagement of the analyte and sample solvent zone decreases with increasing k_m, the period of fast increase of the variance is shorter for larger k_m and the final variance at long migration times is smaller for analytes with larger k_m.
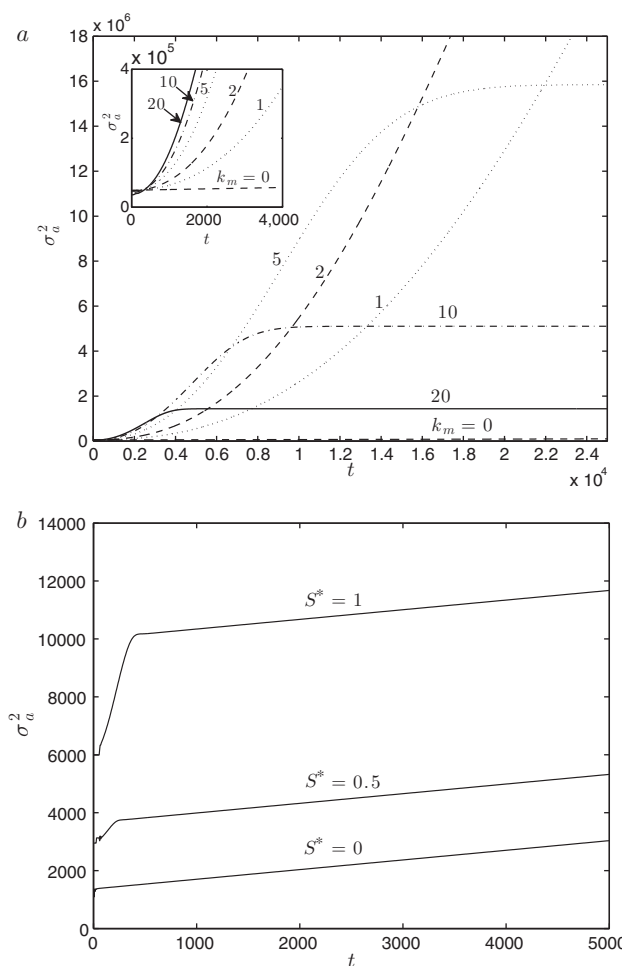
Fig. 8. Temporal evolution of the variance of the axial distribution of the analyte cross-sectional average concentration with $l = 768$, $\delta = 1$, (a) $S^* = 4.8$ and for different values of k_m (insert: enlarged images of early time evolution of variance) and (b) $k_m = 5$, for different values of S^*.

On the other hand, from Fig. 8(b) we found that the total variance of the analyte zone increases with an increase in the sample solvent strength parameter S^*. Also, it is clearly observed that, after the disengagement of the analyte zone from the sample solvent one, the total variance for $S^* = 0.5$ or 1 (which, for $S = 3$, corresponds to a difference in organic modifier composition between the sample solvent and the mobile phase of 7.2% or 14.5%, respectively), increases at the same rate as the variance of the analyte injected in the mobile phase $\sigma_{a,0}^2$, which corresponds to $S^* = 0$ (absence of solvent strength effect). The differences in the initial variance of the various curves of Fig. 8(b) arise from differences in the initial length of the analyte zone, which increases with decreasing k_s, hence with increasing S^*. The amount of variance increase during the transient period reflects the influence of the solvent strength effect.

In order to understand the influence of S^* on the total variance in the transient phase, the contribution arising from the solvent strength effect to the total variance, $\sigma_{a,s}^2$, is plotted in Fig. 9(a)–(c) for different values of k_m, S^* and l, respectively. This variance increases first in a more or less sigmoidal way, due to the solvent strength effect, reflected by a finite value of S^*, before saturating to an asymptotic value after the disengagement of the analyte zone from the sample solvent one. It is seen from Fig. 9(a) that the saturation time of $\sigma_{a,s}^2$ decreases with increasing k_m for fixed value of S^*. On the other hand, this saturation time increases with increasing S^* as well as with increasing l for a fixed value of k_m (see Fig. 9(b) and (c)).
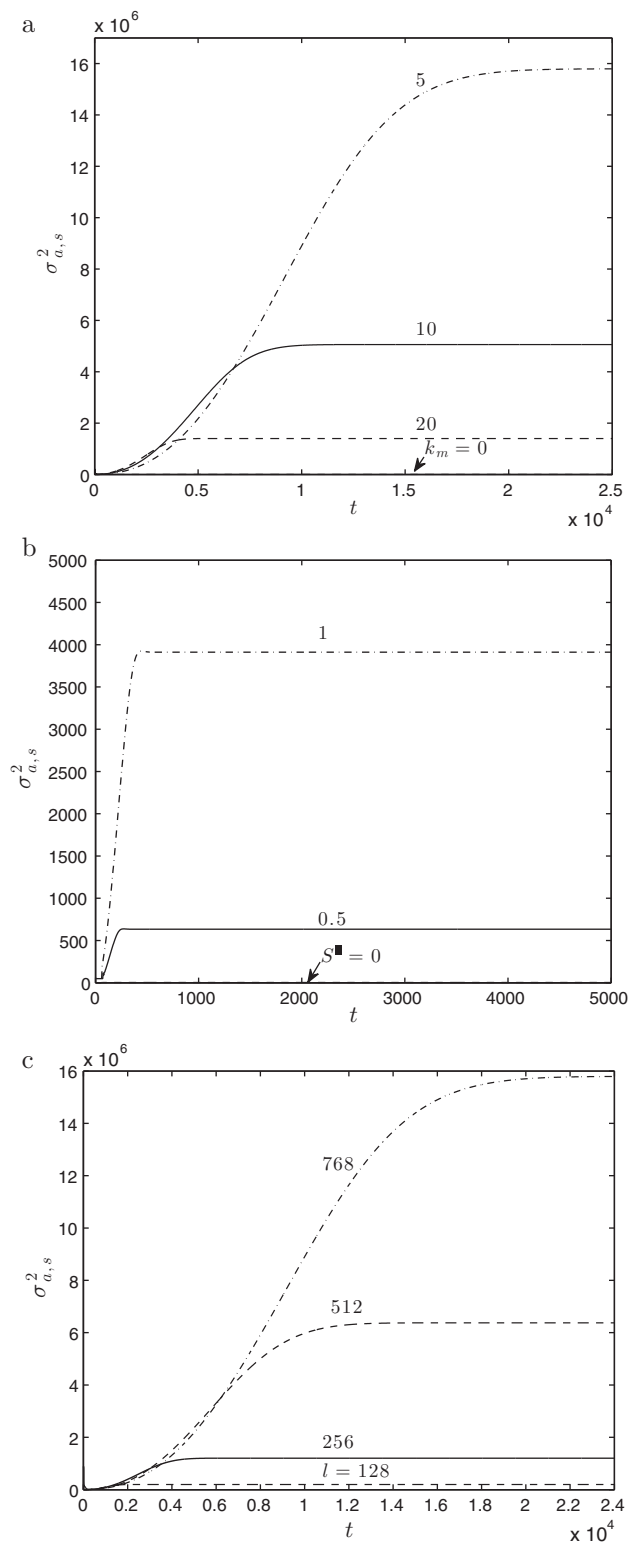

Fig. 9. Temporal evolution of the contribution of solvent strength effect to the analyte variance $\sigma_{a,s}^2$ with $\delta = 1$, (a) for different values of k_m with $S^* = 4.8$, $l = 768$, (b) for different values of S^* with $k_m = 5$, $l = 768$, and (c) for different values of l with $S^* = 4.8$, $k_m = 5$.

These findings are in agreement with the results of the simplified model of the critical time exhibited in Fig. 6. This model is based on the assumption of no dispersion of the sample solvent zone. Therefore, its results cannot match exactly those of the simulation data in which the dispersion of the sample solvent zone is accounted for. It

is interesting to note that the critical time is in fact larger than the saturation time observed in Fig. 9. For example when $k_m = 5$, $S^* = 4.8$, t_{crit} (from Eq. (20) and Fig. 6) is found to be 31×10^3, while the corresponding saturation time is approximately equal to 24×10^3 (see Fig. 9(a)). This might appear counter-intuitive since the dispersion of the sample solvent zone extends the length occupied by this zone, and thus could contribute to delay the disengagement of the analyte and sample solvent zone. However, this sample solvent dispersion is accompanied by a decrease of the relative amount of the sample solvent in its mixture with the mobile phase, i.e. of c, and, thus by a decrease in the "force" pulling the analyte zone ahead of the space it would occupy if it was entirely surrounded by the mobile phase. This reduced "force" effect appears to overcome the dispersion effect.

The influence of the sample volume, reflected into the non-dimensional length occupied by the sample solvent in the column, l, is quite significant, as seen in the plots of the temporal evolution of the contribution of the solvent strength effect on the spatial variance of the analyte zone in Fig. 9(c), for different values of $l = 128$, 256, 512 and 768. For an analyte with a reduced plate height of 3, these l values correspond to injection volumes of 6.7 µL, 13.4 µL, 27 µL and 40 µL, respectively, for a 4.6 mm i.d. HPLC column packed with 3 µm particles, and of 0.8 µL, 1.6 µL, 3.2 µL and 4.7 µL for a 2.1 mm i.d. very high pressure LC column packed with 1.7 µm particles, when the total porosity is 0.7. The saturation time t_{sat}, defined as the time at which $\sigma^2_{a,s}$ reaches 99.9% of its saturation value, increases approximately linearly with increasing l (see Fig. 10(a)), in agreement with the trend found for the dependence of the critical time on l in Fig. 7. However, the saturation value of $\sigma^2_{a,s}$ (i.e. σ^2_{a,s_∞}) increases by a factor 6, 32 or 80 when l increases from 128 by a factor 2, 4 or 6, respectively, i.e. approximately as $l^{2.4}$ as shown in Fig. 10(b). The value of the exponent of such a power law should however be taken with care as more data are needed to confirm its value. Anyway, this illustrates the strong dependence of the peak variance (at saturation, i.e. after disengagement of the sample solvent and analyte zones) on the injected sample volume.

3.4. Skewness of the analyte distribution

The third moment, i.e. the skewness, of the analyte cross-sectional average concentration is given by [39]

$$a(t) = \frac{\int_0^L (1 + k(c)) c_{a,m}(x, t)[x - m(t)]^3 dx}{\int_0^L (1 + k(c)) c_{a,m}(x, t) dx} \quad (22)$$

It provides information about the symmetry of the peak with respect to its mean position. In Fig. 11, $a(t)$ is plotted as a function of t for different values of k_m. The skewness becomes non zero due to the asymmetry of the distribution of the analyte with respect to the mean position. Whatever k_m, it is observed that, at early times, the skewness is negative. Then, after a while, it reverts to positive values and finally saturates to a maximum positive value. This change in skewness is observed at three critical times t_1, t_2 and t_3, corresponding to the three different properties of the analyte skewness, i.e. global minimum, sign reversal and saturation respectively. For example, with $k_m = 5$, the skewness attains the global minimum at $t_1 \simeq 9000$, zero at $t_2 \simeq 12,000$ and the saturation time $t_3 \simeq 24,000$. In order to investigate this behavior at these indicative times a close study of the analyte cross-sectional average concentration profile, proportional to $(1 + k(c)) c_{a,m}$, is plotted in Fig. 12 for a fixed retention factor $k_m = 5$.

Generally speaking, for a monomodal distribution of a quantity, y, as a function of a variable, x, the skewness is positive when the distribution is more tailing in the direction of large x values than in the direction of small x values, and it is negative in the opposite case. The situation is more complicated for bimodal distributions as
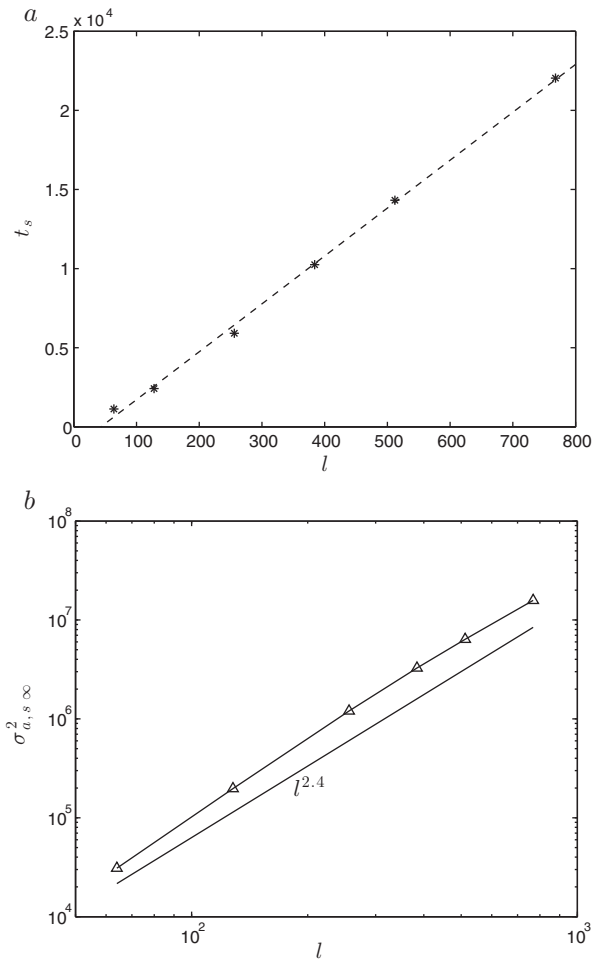

Fig. 10. (a) Saturation time t_{sat} of the analyte variance $\sigma^2_{a,s}$ for different l with $k_m = 5$ and $S^* = 4.8$. (b) Log–log plot of saturation analyte variance σ^2_{a,s_∞} as a function of l with $k_m = 5$ and $S^* = 4.8$. The straight line with label $l^{2.4}$ is shown as a reference for a power law with exponent 2.4 relating σ^2_{a,s_∞} to l.

is the case here. Nevertheless, at early times, because a significant amount of analyte is located in the high and fine peak near $x = 0$ in the moving frame of reference, the distribution tails essentially in the left, upstream part of the x axis and the skewness is increasingly
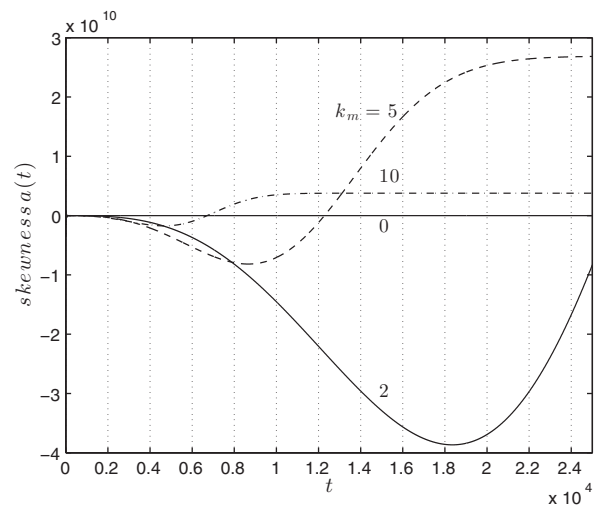

Fig. 11. Temporal evolution of the skewness of the axial distribution of the analyte cross-sectional average concentration with $l = 768$, $S^* = 4.8$ for different values of k_m.
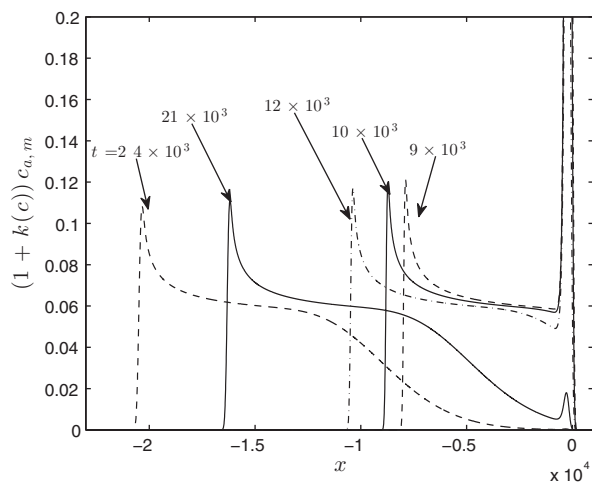
Fig. 12. Analyte cross-sectional average concentration profile, proportional to of $(1 + k(c))c_{a,m}$, at the times at which the skewness shows a change in behavior for $k_m = 5$ and $S^* = 4.8$ (enlarged).

negative as the upstream interface of the analyte zone goes into more negative values of x. This occurs until t = about 9000. For $t > t_1 (\simeq 9000)$, a small kink starts to appear between the two modes of the distribution. Although this is not visible on the scale of Fig. 12, it is accompanied by a decrease of the amplitude of the downstream mode near $x = 0$. Consequently, the skewness becomes less negative until at, some time, t_2, it becomes zero, although the profile of the analyte zone is not symmetric. Later on, the downstream mode becomes smaller and smaller, as seen at t = 21,000, and the upstream mode is dominating. Then, the distribution profile of the analyte cross-sectional average concentration is essentially tailing on the downstream side (large x values, although these values are negative in the moving frame of reference) and the skewness is then positive. The time t_3 clearly corresponds to the disappearance of the first, downstream mode, when the analyte and sample solvent zones are disengaged, i.e. to the saturation time discussed earlier for the variance (see Fig. 8, $k_m = 5$). It should be noticed that we discuss here the skewness of the analyte distribution along the column. The results would be different if we were discussing the skewness of the temporal distribution of the analyte at the column outlet. Indeed, a zone exhibiting an upstream tail (with a negative skewness of its spatial distribution) would lead to an elution curve tailing on the long time side with a positive skewness of its temporal distribution. This is because smaller migration distances are associated to longer elution times.

3.5. Spreading length of the analyte

The influence of the solvent strength of the sample solvent on the dispersion dynamics of the analyte is also witnessed in the spreading length of the solute zone. This spreading length is quantified by the length l_d of the interval in which $c_{a,m}(x, t) > 0.001$ [24,25]. The evolution of the spreading length of the solute defined as $L_d = l_d − l_a$, is plotted in Fig. 13 for different values of S^* with retention factor $k_m = 1$. It is noted that due to the presence of the non-isoeluotropic sample solvent, the temporal dependence of the spreading length departs from that observed for $S^* = 0$ in the pure dispersive regime. For small S^*, the spreading length is seen to exhibit a similar trend. However, for $S^* = 1$ or 2, the growth rate of the spreading length increases with increasing S^* and exhibits a discontinuity at a time which also increases with S^*. In order to get more insight in the influence of the solvent effect on the spreading length of the analyte, the corresponding log–log plot of L_d versus t is depicted in Fig. 13(b). For $S^* = 0$ the spreading length evolves
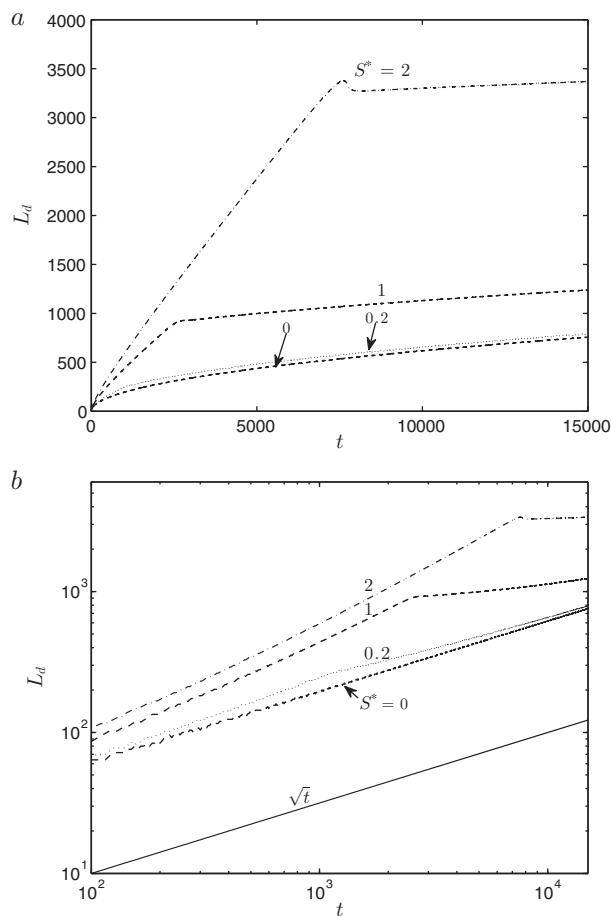

Fig. 13. (a) Spreading length of the analyte zone as a function of t for different values of S^* with $k_m = 1$, $l = 768$ and $\delta = 1$, (b) corresponding log–log plot of (a) and the solid line depicts the characteristic slope corresponding to pure dispersive analyte spreading length without adsorption.

proportionally to $\sqrt{t}$ as observed in Mishra et al. [24]. The discontinuity noticed above is clearly apparent for $S^* = 1$ or 2 but even also for $S^* = 0.2$. The discontinuity point corresponds to the saturation time when the analyte and sample solvent zones become disengaged. Before that time, the analyte zone spreads with a power of t which is greater than 0.5 and which increases with increasing S^*.

4. Conclusions

The sorption of an analyte on the stationary phase, with retention factor k depending on the concentration of the sample solvent in the mobile phase, affect its transport dynamics. When the sample solvent is a stronger eluent than the mobile phase, the analyte concentration along the chromatographic column features a bimodal distribution curve depending on a parameter S^* which is proportional to the solvent strength parameter S and to the difference in organic modifier content between the sample solvent and the mobile phase. Due to the solvent strength effect, such a deformation of the analyte zone occurs because the downstream part of this zone moves at a relatively high velocity with a low retention factor in the sample solvent while the rear, upstream, part of the zone, more retained in the carrier liquid, moves at a relatively low velocity. Thus the presence of a strong sample solvent contributes to increase the width of the analyte zone well above that arising from the chromatographic migration in a liquid environment of constant composition. The magnitude of this solvent strength effect depends strongly on the sample volume. While

understanding quantitatively its influence on the dispersion of the analyte is important for the optimization of the chromatographic separation, it is particularly so in the case of comprehensive two-dimensional LC where relatively large volume fractions collected from the effluent of the first column are injected in the second column operated with a mobile phase of different composition [50,51].

The present study provides some insight in this regard. It has to be recalled that the analyte sorption isotherm has been assumed to be linear. The situation is more complex for non-linear isotherms [52]. Furthermore, we have assumed that the sample solvent or the organic modifier is not retained by the stationary phase, which is a valid assumption for methanol or acetonitrile in RPLC. When it is not so, it is observed that the analytes moving faster than the sample solvent are not affected by the solvent strength effect [48].

The solvent strength effect described above is sometimes called the breakthrough effect in reference to a somewhat similar phenomenon observed in the chromatographic analysis of polymers [53]. Indeed, in some conditions, two separated peaks may be observed for a single narrow polymer standard, their relative amount depending on the difference in solvent strength between the sample solvent and of the mobile phase as well as on the sample volume [54]. However, the results of our present study correspond primarily to the reversed-phase liquid chromatographic behavior of relatively small analytes and cannot be thought as describing that of macromolecular species.

As mentioned above, a difference in viscosity is likely to be associated to a difference in solvent composition between the mobile phase and the sample solvent. Therefore, the present analysis of the sole effect of solvent strength on the dynamics of the analyte is a first step before investigating the combined influences of the viscosity and solvent strength effects on the analyte dispersion. This will be the topic of a forthcoming publication. Although the simulations performed in this study exhibit spatial analyte distributions along the column rather than related, but somewhat different, temporal distributions at the column outlet, they illustrate and allow to understand a variety of experimental situations observed for peaks in chromatograms when analytes are injected in a sample solvent stronger than the mobile phase.

Acknowledgement

References

[1] C.-Y. Wu, J.J. Wittick, Anal. Chim. Acta 79 (1975) 308.
[2] P.K. Tseng, L.B. Rogers, J. Chromatogr. Sci. 16 (1978) 436.
[3] J. Kirschbaum, S. Perlman, R.B. Poet, J. Chromatogr. Sci. 20 (1982) 336.
[4] M. Tsimidou, R. Macrae, J. Chromatogr. 285 (1984) 178.
[5] M. Tsimidou, R. Macrae, J. Chromatogr. Sci. 23 (1985) 155.
[6] F. Šhakik, G.B. Beecher, J.T. Vanderslice, G. Furrow, Anal. Chem. 60 (1988) 807.
[7] N.E. Hoffman, S.-L. Pan, A.M. Rustum, J. Chromatogr. 465 (1989) 189.
[8] D. Vukmanic, M. Chiba, J. Chromatogr. 483 (1989) 189.
[9] J. Layne, T. Farcas, I. Rustamov, F. Ahmed, J. Chromatogr. A 913 (2001) 233.
[10] E.S. Kozlowski, R.A. Dalterio, J. Sep. Sci. 30 (2007) 2286.
[11] J. Ruta, S. Rudaz, D.V. Mc Calley, J.-L. Veuthey, D. Guillarme, J. Chromatogr. A 1217 (2010) 8230.
[12] E.L. Johnson, R. Stevenson, Basic Liquid Chromatography, Varian, Palo Alto, 1978, pp. 226.
[13] L.R. Snyder, J.J. Kirkland, Introduction to Modern Liquid Chromatography, 2nd ed., Wiley, New York, 1979, pp. 298.
[14] C.F. Poole, The Essence of Chromatography, Elsevier, Amsterdam, 2003, pp. 443.
[15] G. Rousseaux, A. De Wit, M. Martin, J. Chromatogr. A 1149 (2007) 254.
[16] R.C. Castells, C.B. Castells, M.A. Castillo, J. Chromatogr. A 775 (1997) 73.
[17] D. Cherrak, E. Guernet, P. Cardot, C. Herrenknecht, M. Czok, Chromatographia 46 (1997) 647.
[18] C.B. Castells, R.C. Castells, J. Chromatogr. A 805 (1998) 55.
[19] K.J. Mayfield, R.A. Shalliker, H.J. Catchpoole, A.P. Sweeney, V. Wong, G. Guiochon, J. Chromatogr. A 1080 (2005) 124.
[20] S. Keunchkarian, M. Reta, L. Romero, C. Castells, J. Chromatogr. A 1119 (2006) 20.
[21] H.J. Catchpoole, R.A. Shalliker, G.R. Dennis, G. Guiochon, J. Chromatogr. A 1117 (2006) 137.
[22] R.A. Shalliker, G. Guiochon, J. Chromatogr. A 1216 (2009) 787.
[23] W. De Malsche, J. Op De Beek, H. Gardeniers, G. Desmet, J. Chromatogr. A 1216 (2009) 5511.
[24] M. Mishra, M. Martin, A. De Wit, Phys. Fluids 21 (2009) 083101.
[25] M. Mishra, M. Martin, A. De Wit, Chem. Eng. Sci. 65 (2010) 2392.
[26] G. Rousseaux, M. Martin, A. De Wit, J. Chromatogr. A 1218 (2011) 8353.
[27] J. Lankelma, H. Poppe, J. Chromatogr. 149 (1978) 587.
[28] J.C. Kraak, F. Smedes, J.W.A. Meijer, Chromatographia 13 (1980) 673.
[29] P.R. Guinebault, M. Broquaire, R.A. Braithwaite, J. Chromatogr. 204 (1981) 329.
[30] P.R. Guinebault, M. Broquaire, J. Chromatogr. 217 (1981) 509.
[31] K. Šlais, D. Kouřilovà, M. Krejči, J. Chromatogr. 282 (1983) 363.
[32] H.A. Claessens, M.A.J. Kuyken, Chromatographia 23 (1987) 331.
[33] M.J. Mills, J. Maltas, W.J. Lough, J. Chromatogr. A 759 (1997) 1.
[34] A. Cappiello, G. Famiglini, A. Berloni, J. Chromatogr. A 768 (1997) 215.
[35] J.P.C. Vissers, H.A. Claessens, C.A. Cramers, J. Chromatogr. A 779 (1997) 1.
[36] S. Héron, A. Tchapla, J.-P. Chervet, Chromatographia 51 (2000) 495.
[37] A.C. Sanchez, J.A. Anspach, T. Farkas, J. Chromatogr. A 1228 (2012) 338.
[38] J.W. Dolan, L.R. Snyder, Troubleshooting LC Systems, Humana Press, Clifton, 1989, pp. 268.
[39] A. De Wit, Y. Bertho, M. Martin, Phys. Fluids 17 (2005) 054114.
[40] M. Mishra, M. Martin, A. De Wit, Phys. Fluids 19 (2007) 073101.
[41] M. Mishra, M. Martin, A. De Wit, Phys. Rev. E 78 (2008) 066306.
[42] T.-L. Ng, S. Ng, J. Chromatogr. 329 (1985) 13.
[43] G. Guiochon, A. Felinger, D.G. Shirazi, A.M. Katti, Fundamentals of Preparative and Nonlinear Chromatography, Elsevier – Academic Press, San Diego, 2006.
[44] L.R. Snyder, J.W. Dolan, J.R. Gant, J. Chromatogr. 165 (1979) 3.
[45] J.W. Dolan, J.R. Gant, L.R. Snyder, J. Chromatogr. 165 (1979) 31.
[46] C.T. Tan, G.M. Homsy, Phys. Fluids 31 (1988) 1330.
[47] L.N. Trefethen, Finite Difference and Spectral Methods for Ordinary and Partial Differential Equations, unpublished text, available from http://people.maths.ox.ac.uk/trefethen/pdetext.html (1996).
[48] E. Loeser, P. Drumm, J. Sep. Sci. 29 (2006) 2847.
[49] N.S. Patil, R.B. Mendhe, A.A. Sankar, H. Iyer, J. Chromatogr. A 1177 (2008) 234.
[50] R.A. Shalliker, G. Guiochon, Analyst 135 (2010) 222.
[51] J. Haun, T. Teutenberg, T.C. Schmidt, J. Sep. Sci. 35 (2012) 1723.
[52] K. Gedicke, D. Antos, A. Seidel-Morgenstern, J. Chromatogr. A 1162 (2007) 62.
[53] H.J.A. Philipsen, B. Klumperman, A.M. van Herk, A.L. German, J. Chromatogr. A 727 (1996) 13.
[54] X. Jiang, A. van der Horst, P.J. Schoenmakers, J. Chromatogr. A 982 (2002) 55.